



Contents lists available at <http://qu.edu.iq>

Al-Qadisiyah Journal for Engineering Sciences

Journal homepage: <https://qjes.qu.edu.iq>



Investigation on aerodynamic performance of H-type darrius vertical axis wind turbine with different series airfoil shapes

Sivan Karima Arif  ^{a*} and Iyd Eqqab Maree  ^b

^aMechanical Engineering Department, College of Engineering, Salahaddin University Erbil, Iraqi Kurdistan, Iraq

^bAviation Engineering Department, College of Engineering, Salahaddin University Erbil, Iraqi Kurdistan, Iraq

ARTICLE INFO

Article history:

Received 25 December 2022

Received in revised form 05 March 2023

Accepted 18 June 2023

Keywords:

H-type

DMST

Power Coefficient

Tip Speed

Self-starting

ABSTRACT

Wind energy is one of the most important renewable energies since it reduces environmental pollution. Darrius VAWTs with straight blades are more prevalent in small-scale power generation due to their simple blade design and easy construction. The investigation of the performance of VAWTs is a topic that is fascinating for researchers to look into. Researchers have paid special attention to the Double Multiple Stream tube (DMST) models for VAWT simulation because of the good correlation between the DMST model and the experimental results. In this paper, double multiple stream-tube analysis is performed using MATLAB programming to predict the aerodynamic performance of H-type Darrius fixed pitch VAWT, more specifically, the power coefficient (C_p) and the tip speed ratio (TSR). The fact that the H-type Darrius rotor has poor self-starting despite having a good power coefficient which is a constant worry at low wind speeds. The selection of the air foil is one of the most essential factors to take into account while trying to enhance the aerodynamic performance of H-type Darrius fixed pitch VAWT. In this study, first, results from experiments were used for the validation of the model, and then, 4 different families of symmetrical air foils were compared. The results indicate that the symmetrical air foil S-1046 showed exceptional aerodynamic performance and a high starting torque for a low wind speed of 4 m/s.

© 2023 University of Al-Qadisiyah. All rights reserved.

1. Introduction

In the current world of technological advancements, innovations, and inventions, industrialization is reaching new heights. Technological progress is inextricably linked to the use of energy. In contrast, rapid industrialization has created a slew of problems and challenges that are far too significant to ignore now. The issues to be considered are increasing air pollution, rising fuel costs, massive energy consumption in various industries, etc. [1]. The selection of suitable alternative energy sources is a significant issue impacting economic growth worldwide. The wind is considered a source of alternative energy because it is renewable, economically competitive, relatively clean, and environmentally friendly.

Wind technology transforms kinetic energy from the wind into mechanical or electrical power through wind turbines (WTs) using aerodynamically designed blades [2]. WTs can be divided into two categories, horizontal axis wind turbines (HAWTs) and vertical axis wind turbines (VAWTs), depending on the orientation of the axis of alignment [3]. HAWTs rotational axes are parallel to the wind stream, and they were a popular choice due to their better aerodynamic behaviour and efficiency on a large scale. In contrast, VAWTs' rotational axes are perpendicular to the wind stream. VAWTs have many benefits that guide researchers' attention. VAWTs are omnidirectional without needing a yaw system, which results

* Corresponding author.

E-mail address: seevan.kareem@gmail.com (Sivan Karima)

<https://doi.org/10.30772/qjes.v16i2.881>

2411-7773/© 2023 University of Al-Qadisiyah. All rights reserved.



This work is licensed under a Creative Commons Attribution 4.0 International License.

Nomenclature:

a_{up}, a_{do}	Upstream and downstream interference factor	V_{up}, V_{do}	Upstream and downstream induced velocity
c	Blade chord	V_e	Equilibrium induced velocity
C_d	Drag coefficient	V_o	Ambient airspeed
C_l	Lift coefficient	$V_{r,up}, V_{r,do}$	Upstream and downstream resultant air velocity
$C_{N,up}, C_{N,do}$	Upstream and downstream normal coefficient	X	Rotor tip speed ratio
$C_{p'}, C_{P_{up}}, C_{P_{do}}$	Power coefficient, upstream and downstream	X_{up}, X_{do}	Upstream and downstream local tip speed ratio
$C_{Q_{up,av}}$	Average torque coefficient	<i>Greek symbols</i>	
$C_{T,uw/a}, C_{T,do}$	Tangential coefficient	α_{up}, α_{do}	Upstream and downstream angle of attack
$Z + Q_{av}, Q_{up,av}, Q_{do,av}$	Average torque, upstream and downstream	α_o	Initial angle of attack
Q_{up}	Upstream torque	ν	Air kinematic viscosity
F_{up}, F_{do}	Function characterizing upstream and downstream flow conditions	π	Pi
$F_{N,up}$	Normal force	θ	Azimuth angle
$F_{T,up}$	Tangential force	ρ_a	Air density
L	Blade length	σ	Solidity
N_b	Blades number	ω	Rotor angular speed
R	Rotor radius		
Re_b	Blade's local Reynolds number		
Y	non-dimensional Y-coordinates		
S	Swept area		

in fewer hydrodynamic motions and platform design constraints. The generator location of VAWTs differs from that of HAWTs, which are located at the base of the tower, reducing the load on the tower. This type of design has a direct effect on the turbine's easy maintenance, construction, and installation [4]. Many VAWT designs have been created over the years and can be categorized into drag-type (Savonius VAWTs, which are the simplest sort) and lift-type (Darrius VAWTs, which are more complicated) based on rotation-driving aerodynamic forces [5].

Typically, there were two types of Darrius rotors: curved and straight-bladed. Darrius VAWTs with curved blades have lower bending stress in the blades than Darrius VAWTs with straight blades; hence, they are more economically successful [6]. However, Darrius VAWTs with straight blades are more common in small-scale power generation due to the ease of their blade design [7]. Straight-blade VAWTs are Darrius VAWTs with straight blades instead of curved blades. As a result of its rotor aspect, it is always referred to as H-rotor [8]. In recent years, H-type Darrius VAWTs are getting more notice in the field of wind energy. In many countries, H-type Darrius sVAWTs are actively researched and promoted. They work well in turbulence and different environments and regions [9]. Darrius VAWTs have complex aerodynamic behavior, but different numerical models for performance prediction and design exist. These models are classified as momentum, vortex, and computational fluid dynamics (CFD) models in the literature. For this paper, a momentum model is chosen to predict VAWT's performance using a double multiple stream tube (DMST) models. The momentum models, also known as streamline (ST) models, investigate the dynamic properties of the airflow on the blades and their forces. These models concentrate on the momentum (actuator disk) theory and can be broken down further into the following categories: (single (S), multiple (M), and double multiples (DM)) stream tube models. Templin, R. [10]. Created SST model and calculated momentum balance using a single

stream tube that encompassed the entire turbine, and flow velocities in the stream tube were assumed to be uniform. This model's many assumptions cause inaccurate performance predictions and higher prediction numbers.

Strickland, J. [11]. Developed MST model, which is a more complex analytical method than SST. He assumed that the induced velocity varies vertically and horizontally across the frontal disc area of the rotor. Airfoil geometry, drag forces, curvature flow, etc., have been counted in this model. MST delivers relatively greater accuracy, but it is still insufficient for calculating the aerodynamic blade loads. Paraschivoiu, I. [12]. Developed the DMST model, he assumed that the rotor would behave in the same manner as the actuator disk. The actuator disc is split into two equivalents half cycles, representing the rotor's upstream and downstream sides. DMST model is more precise than MST model. Also, a more accurate agreement between computed and experimental data is seen with the DMST model.

Darrius VAWTs have the highest efficiency value, but they have poor self-starting capability [13], which can be avoided through careful design. Many projects related to the Darrius turbine have been studied through this project to improve and develop the study of the H-type Darrius turbine. Durrani et al. [14]. Compared the performance of NACA 4-digit symmetric airfoils (0012, 0015, and 0018) and NACA 0022 (a thicker air foil size) for a three-blade VAWT at various wind speeds. The results show that, at the various tip speed ratios, NACA0015 gives a more steady performance than the others. Castillo, J. [15], studied many parameters for designing small-scale VAWT with solid wood as a construction material, such as type of blade profile, number of the blade, rotor radius, TSR, and chord length. He used the DMST model for rotor aerodynamic analysis based on a Matlab program. He analyzed the effect of the blade profile on the symmetric NACA0015, and NACA 0021. He concluded that the rotor with the thicker airfoil NACA 00021 has a higher self-starting ability. Mohamed, M. [16]. Studied the aerodynamic performance of the H-rotor Darrius VAWT by using 2D-CFD simulations to study the effect of airfoils on power coefficient. He studied the effects of 20 different airfoils (symmetric and asymmetric) and demonstrated that the use of the symmetric S-1046 airfoil increases the output power of the H-rotor Darrius turbine. Kanyako and Janajreh [17]. Tested different types of airfoils numerically using 2D-CFD simulation for a small-scale VAWT with straight-bladed with a solidity of 0.98 to obtain the best possible performance. They concluded that the best

sectional profile airfoil at low speeds was NACA 0015. Nguyen et al. [18] numerically analyzed the effect of airfoil geometry, the starting azimuth angle of the blade, and wind velocity on self-starting behavior for a 1 KW H-Darrieus rotor with three blades. They analyzed the effect of airfoil thickness on the symmetric NACA 4-digit (0012, 0015, 0018, 0021). They concluded that the H-Darrieus rotor with the thinner airfoil NACA 0012 has a lower self-starting ability, whereas the rotor with the thicker airfoil NACA 00021 has a higher self-starting ability. Subramanian et al. [19]. Numerically investigated the effect of different airfoil profiles on the performance of VAWTs. They discovered that at various tip-speed ratios, different airfoils with different profiles behave differently. Thicker airfoils operate better for lower tip-speed ratios, whereas thinner airfoils work better for higher tip-speed ratios.

In this study, numerical code was developed based on the DMST model with variable interference factors using the MATLAB program to compare the performance and torque characteristics of H-type Darrieus WTs. Although the aerodynamic performance of different airfoil profiles to improve the self-starting performance of small-scale fixed-pitch H-type Darrieus WTs was also studied.

2. Material and method

2.1 Aerodynamic analysis of H-type Darrieus VAWT

DMST model illustrated in Fig. 1 is an analytical model used for Darrieus VAWTs with curved blades for determining aerodynamic blade loads and rotor performance, which was developed by I. Paraschivoiu [20]. The rotor's upstream and downstream sides have their induced velocity. The pressure discontinuity causes the wind speed to slow, resulting in an induced velocity. The upstream-induced velocity V_{up} , which is the axial flow velocity that passes through the stream tubes, and the downstream-induced velocity V_{do} are calculated as follows:

$$V_{up} = a_{up} V_o \quad (1)$$

$$V_{do} = a_{do} V_e \quad (2)$$

where a_{up} and a_{do} are upstream and downstream interference factors, respectively, and it is taken that $(1 > a_{up} > a_{do} > 0)$ and their value drops as the tip speed ratio increases. The value of a_{up} can be determined iteratively by starting with an assumption of $a_{up} = 1$. After that a_{ad} can be determined iteratively starting with $a_{do} = a_{up}$. V_o is ambient air velocity, and V_e is equilibrium velocity at the middle plane, which is affected by the upstream wake velocity: and it is less than V_{up} but greater than V_{do} because the induced velocity in the axial stream tube reduces as given by calculated as follows:

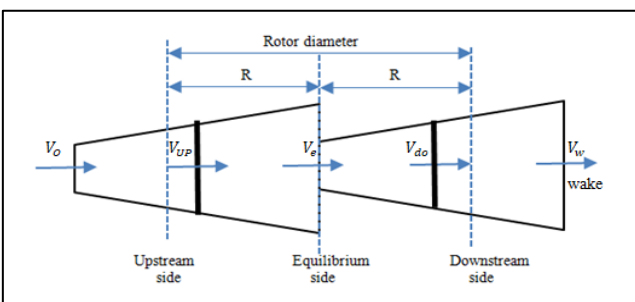


Figure 1. The DMST model is shown schematically.

$$a_{up} = \frac{V_{up}}{V_o} \quad (3)$$

$$a_{do} = \frac{V_{do}}{V_o} \quad (4)$$

$$V_e = \left(2 \frac{V_{up}}{V_o} - 1\right) V_o = (2a_{up} - 1) V_o \quad (5)$$

by substituting equation 5 into equation 2, equation 6 is yield.

$$V_{do} = a_{do} (2a_{up} - 1) V_o \quad (6)$$

the DMST model for H-type Darrieus VAWT, whose illustration is shown in Fig. 2, was adapted based on the following assumptions: (i) assumed that straight vertical blades were subject to the constant flow velocity across the entire length despite the Troposkien-shaped Darrieus turbine used by Paraschivoiu; therefore, angle $(\delta = 0)$. (ii) Assumed that VAWT is fixed-pitch, utilizing symmetric airfoils, where the line of the chord is tangent to the blade flight path, and $\alpha_o = 0$. (iii) 36 stream tubes were employed, meaning wind conditions were evaluated in 5° increments at blade positions. This number was used by Paraschivoiu to present his model's results [21, p. 164]. More stream tubes were tested to examine air conditions in smaller increments; however, the power coefficient and torque didn't change.

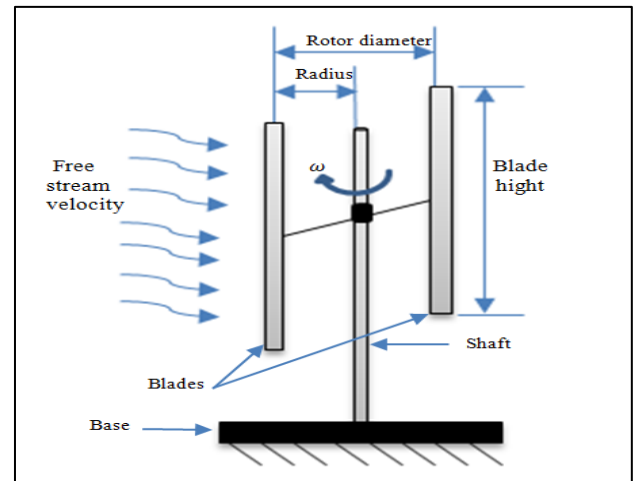


Figure 2. Two-bladed H-type Darrieus

the rotor's upstream side is for Azimuth angles $(-89 < \theta < 89)$. Fig. 3 presents the aerodynamic characteristics of H-type Darrieus VAWT.

The local relative velocity is given by:

$$V_{r,up} = \sqrt{V_{up}^2 [(X_{up} - \sin\theta)^2 + (\cos\theta)^2]} \quad (7)$$

and the upstream local angle attack α_{up} is given by:

$$\alpha_{up} = \sin^{-1} \left[\frac{\cos\theta \cos\alpha_o - (X_{up} - \sin\theta) \sin\alpha_o}{\sqrt{(X_{up} - \sin\theta)^2 + (\cos\theta)^2}} \right] \quad (8)$$

where x_{up} is the local tip speed ratio and calculated as follows:

$$X_{up} = \frac{\omega R}{V_{up}} \quad (9)$$

then the relative velocity $V_{r,up}$ is used to calculate the blade's local Reynolds number Re_b .

$$Re_b = \frac{V_{r,up} c}{\nu} \quad (10)$$

where c is the blade chord and ν is air kinematic viscosity for air at the temperature of 15°C has a reference value of $1.4607 \times 10^{-5} m^2/s$ [22].

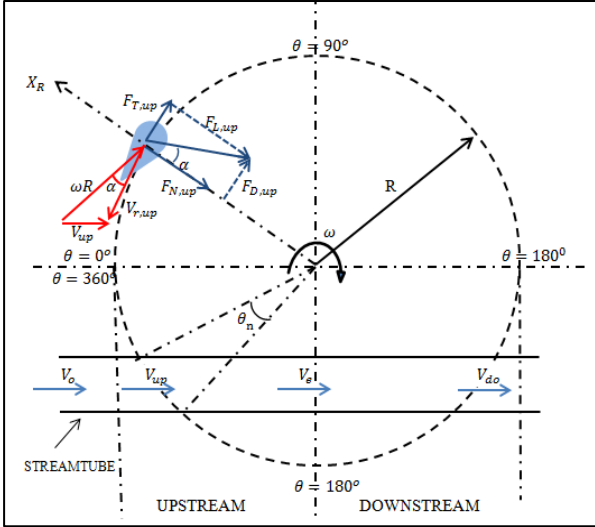


Figure 3. The aerodynamic characteristics of H-type Darrieus VAWT

By using double interpolation, Re_b and α_{up} are utilized to acquire the appropriate drag C_d and lift C_l coefficients.

The lift and drag forces are split into tangential and normal components to determine the amount of torque generated by the blade. The rotor's upstream side normal $C_{N,up}$ and tangential $C_{T,up}$ coefficients are calculated as follows:

$$C_{N,up} = C_l \cos \alpha + C_d \sin \alpha \quad (11)$$

$$C_{T,up} = C_l \sin \alpha - C_d \cos \alpha \quad (12)$$

according to Paraschivoiu, the rotor's upstream side flow conditions can be characterized by F_{up} utilizing the blade element theory in conjunction with the momentum equation.

$$F_{up} = \frac{N_b c}{4\pi \cdot 2R} \int_{-89}^{89} \left| \frac{1}{\cos \theta} \right| (C_{N,up} \cos \alpha + C_{T,up} \sin \alpha) \left(\frac{V_{r,up}}{V_{up}} \right) d\theta \quad (13)$$

where $N_b \cdot c/2R$ represents the solidity, the region of the frontal swept area of the wind turbine covered by the blades and denoted by σ .

The interference factor is then calculated as follows:

$$a_{up} = \frac{\pi}{F_{up} + \pi} \quad (14)$$

the first round of calculations, which include equations 7 through 14, are carried out with ($a_{up}=1$), and then the procedure is repeated with the new value a_{up} until the values of the initial and final a_{up} are similar to each other. After that, Equations (15) and (16) can be used to calculate the normal $F_{N,up}$ and tangential $F_{T,up}$ forces acting on a single blade in a single azimuthal location:

$$F_{N,up}(\theta) = \frac{1}{2} \rho_a c L V_{r,up}^2 C_{N,up} \quad (15)$$

$$F_{T,up}(\theta) = \frac{1}{2} \rho_a c L V_{r,up}^2 C_{T,up} \quad (16)$$

finally, the upstream half-power coefficient $C_{P_{up}}$ is calculating using:

$$C_{P_{up}} = C_{Q_{up,av}} \cdot X \quad (17)$$

where TSR is the tip speed ratio of the rotor, which is calculated as follows:

$$X = \frac{\omega R}{V_o} \quad (18)$$

and $C_{Q_{up,av}}$ the average torque coefficient is calculated as follows:

$$C_{Q_{up,av}} = \frac{Q_{up,av}}{\frac{1}{2} \rho_a S R V_o^3} \quad (19)$$

the rotor's upstream side average torque ($Q_{up,av}$) is given by:

$$Q_{up,av} = \frac{N_b}{2\pi} \int_{-89}^{89} Q_{up}(\theta) d\theta \quad (20)$$

where $Q_{up}(\theta)$ is the torque produced by a blade, which is calculated by combining the lift and torque calculations

$$Q_{up}(\theta) = \frac{1}{2} \rho_a c R L C_{T,up} V_{r,up}^2 \quad (21)$$

The downstream side of the rotor is for the azimuth angle ($91 < \theta < 269$) and using the same set of formulas, the average torque and power coefficient for the rotor downstream side are calculated as follows:

- Using V_{do} instead of V_{up} , the downstream local relative velocity $V_{r,do}$, local angle of attack α_{up} , and local tip speed ratio X_{do} can also be determined from equations 7, 8, and 9.
- Using double interpolation, Re_b and α_{do} are utilized to obtain the appropriate drag C_d and lift C_l coefficients.
- Calculating downstream normal coefficients $C_{N,do}$ and tangential coefficients $C_{T,do}$.
- The downstream interference factor a_{do} can be calculated after calculating the downwind flow conditions F_{do} . The above procedure is repeated with the new value of a_{do} until the initial and final a_{do} values are similar.
- The average torque $Q_{do,av}$ and power coefficient $C_{P_{do}}$ on the downstream side are being calculated.

finally, the rotor's average torque and total power coefficient C_{P_t} are calculated by summing the two contributions:

$$Q_{av} = Q_{up,av} + Q_{do,av} \quad (22)$$

$$C_{P_t} = C_{P_{up}} + C_{P_{do}} \quad (23)$$

2.2 Numerical procedure

For the above referred for calculating aerodynamic loads, average torque Q_{av} , and total power coefficient C_{P_t} , a program code is developed by using MATLAB R2020a. Fig. 4 represents the procedure used for determining the torque and power coefficient for each blade position. The algorithm has 5 input design parameters of the rotor which are (rotor radius (R), blade length (L), number of the blade (N_b), chord length (c), blade profile), ambient air velocity (V_o), and rotational speed (ω). Also, input from the airfoil's data table such as lift and drag coefficient on Reynolds number and angle of attack is imported to the program to calculate rotor lift and drag coefficient by double interpolation. The value of airfoils data C_l

and C_d in a different range of the Reynolds number (1, 8, 16, 36, 70, and 100×10^4 and angle of attack from -180 to 180 degrees obtained from QBlade software. Were C_l and C_d extrapolated with the Montgomerie method, with a CD90 at (1.6) value. Dynamic stall effects are not modeled present analysis code using DMST models. The average torque Q_{av} and total power coefficient C_{P_t} are the algorithm output captured by the integration of all the blade positions.

3. Results and discussion

3.1 Verifying the Model

For the validation of the model, two cases of WTs were used. The rotor's parameter of the two types of turbines used to validate the model is given in Table 1. The reference data value was obtained by reading the plot using DigitizeIt software because the numerical results were unavailable. In case I when comparing the present code analysis with the experimental analysis available in Ref. [23] shown in Fig. 5 it can be noticed that they match at low TSR but overshoot at higher TSR. There is an increasing difference between power coefficient values starting from TSR 2.5 until TSR 3.3, where the biggest difference in the value of Cp is 0.1633 at TSR equal to 3.3. Nevertheless, the results from the experiment by Raciti Castelli, Englaro, and Benini in 2011 were an average of Cp, indicating that the experiment was conducted in multiple sets or trials. Since the real value of Cp can vary on those varying trials or sets, this can affect the experimental graph analysis's shape as well. In conclusion, the differences are still acceptable for both graphs since the two graphs no differ by more.

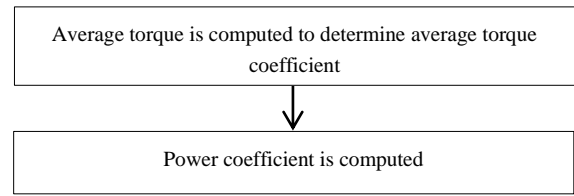
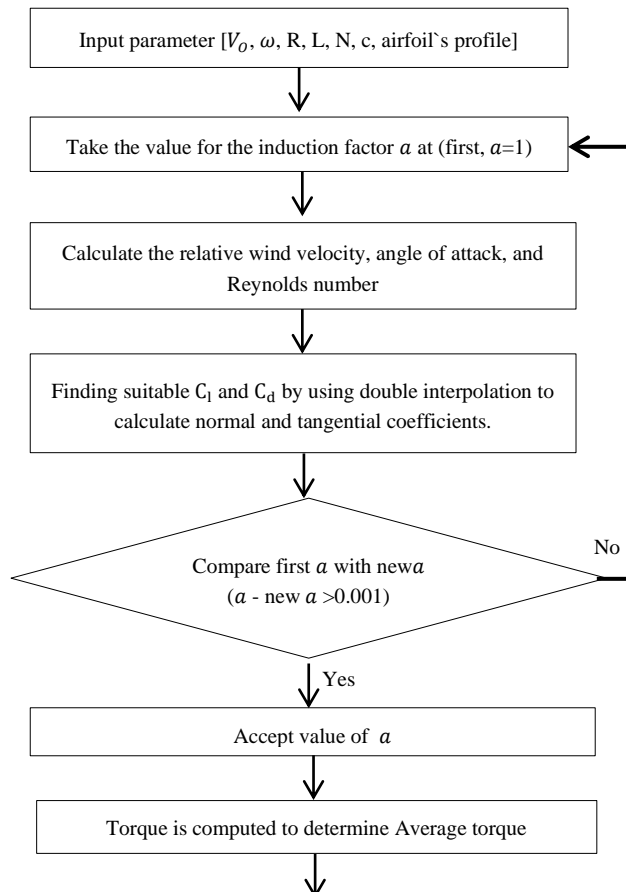


Figure 4. The procedure used for determining the torque and power coefficient for each blade position.

Table 1. Rotor's parameters case I [23] and case II [24]

Rotor parameters	Case I	Case II
Blade profile	NACA0021	NACA0015
Blade number	3	2
Blade height	1.4564	6
Rotor radius	0.515	3
Chord length	0.0858	0.2
Test	V=9m/s	N=125rpm

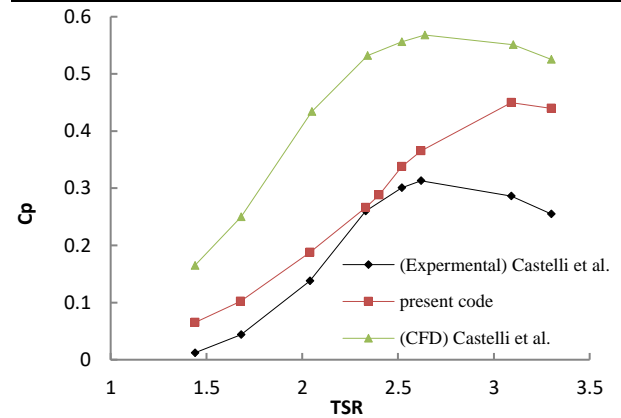


Figure 5. Comparison DMST analysis code with experimental and numerical analysis (case I)

In contrast, the present code analysis graph and numerical analysis show a smaller difference at higher TSR. At TSR 2.33 the value of Cp is 0.2465 which is the biggest value of cp between the present code analysis and numerical analysis than 0.2Cp, and most importantly the two graphs are remarkably similar in shape.

In case II when comparing the present code analysis with the experimental analysis in Ref. [24] shown in Fig. 6 it can be noticed that the obtained result is great, where two graphs are similar in terms of their shape and curves as shown in Fig. 2. Both graphs peak at TSR 4.98 with the difference of 7.3%. In addition, the differences between them are very little and neglectable. In conclusion, the graph curve of the present code analysis simulation can replicate the shape from both numerical and experimental analysis and results agree well with those from other methods based on a variety of published findings. This can ensure that the present code analysis

using the DMST model provides a good and trusted result to evaluate the performance of H- the type Darrieus wind turbine.

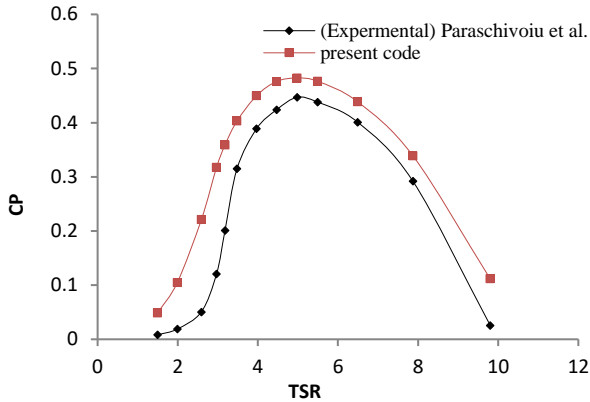


Figure 6. Comparison DMST analysis code with experimental (case II)

3.2 Blade profile

Many parameters, such as type of blade profile, number of the blade, rotor radius, blade length, chord length, and so on, affect the performance of H-type Darrieus WTs. The blade profile selection is the most critical parameter to improve the aerodynamic performance with the ability to self-start without needing additional components [25]. During the optimization process, the Blade profile’s impact on the power coefficient was considered, and the result is shown in the graphs. The simulation was conducted for four families of symmetric airfoils at low wind speed 4m/s and the results for the power coefficients of these profiles at different TSRs are shown. In this study, the chosen swept area will be 1.1 m². The characteristics of the H-type Darrieus wind turbine used for the present study using the DMST model are listed in Table 2.

Table 2. Characteristics of H-type Darrieus WT used for the present study.

Rotor radius (R)	0.6875m
Blade height (L)	0.80m
Swept area (S)	1.10m ²
Blade chord (c)	0.20m
Number of the blade (N _b)	4.00
TSR	2.00
Air velocity (V ₀)	4.00m/s

3.2.1 NACA –Family

In this family, compared the performance of NACA 4-digit symmetric airfoils (0012, 0015, 0018, 0021, and 0024) as shown in Fig. 7, NACA 0018 has the maximum power coefficient of 0.295 at TSR 2. Also, NACA 0018

has a higher self-starting ability compared with other airfoils in the NACA family.

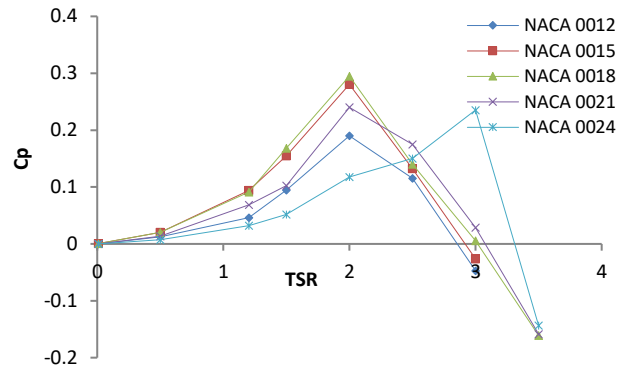


Figure 7. Cp vs. TSR for NACA-Family

3.2.2 S-Family

In this family, compared the performance of symmetric airfoils (S1014, S1016, S1046, and S1048) as shown in Fig. 8 it can be seen that S1046 has a maximum power coefficient of 0.3342 at TSR 2 and has a higher self-starting ability compared with other airfoils in S-families.

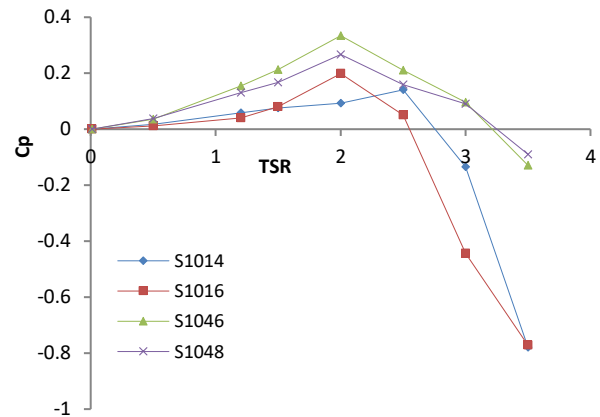


Figure 8. Cp vs. TSR for S-Family

3.2.3 FX-Family

In this family, compared the performance of symmetric airfoils (FX 76-100, FX 76-120, FX 77080, FX 70-L-100, and FX 79-L-120) as shown in Fig. 9 it can be seen that FX-76-120 has a maximum power coefficient 0.2657 at TSR 2 and has a higher self-starting ability compared with other airfoils in FX-families.

3.2.4 E-Family

In this family, compared the performance of symmetric airfoils (E168, E169, E171, E474, and E475) as shown in Fig. 10 it can be seen that E169 has a maximum power coefficient of 0.3017 at TSR 2 and has a higher self-starting ability compared with other airfoils in E-families.

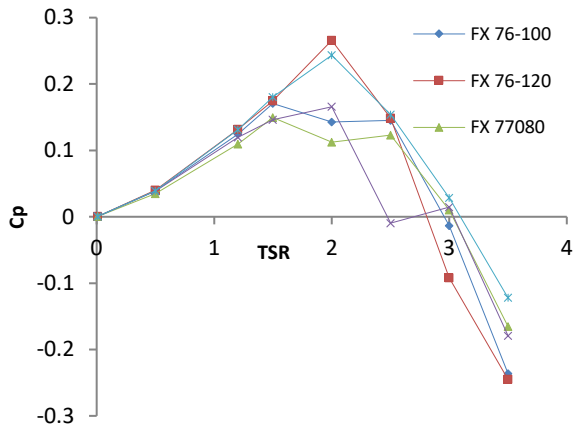


Figure 9. Cp vs. TSR for FX-Family

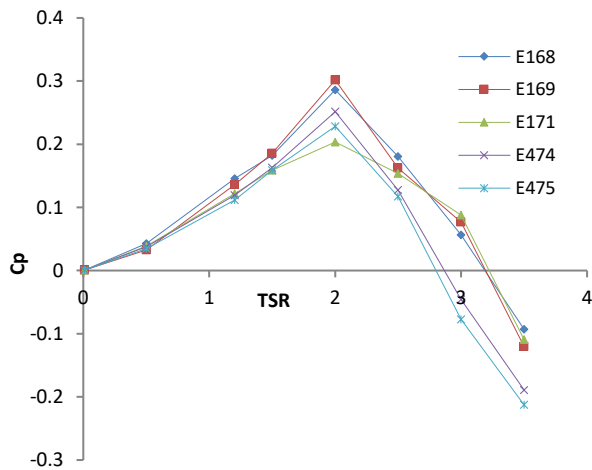


Figure 10. Cp vs. TSR for E-Family

Clearly, after reviewing all figures, it appears that Fig. 7, 8, 9, and 10 are those for airfoil families with the symmetrical profile section. The following Fig. 11 presents the best curve of the airfoil used in this analysis.

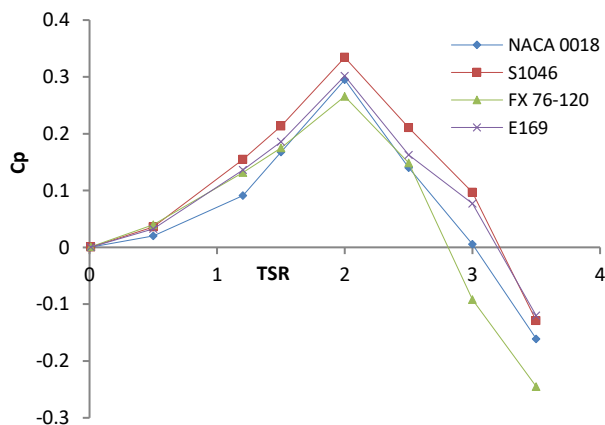


Figure 11. Cp vs. TSR for (1) NACA 0018 (2) S1046 (3) FX 76-120 (4) E169 rotors

It clearly shows that the symmetrical airfoil section s1046 is the best compared with other airfoils (NACA 0018, E169, and FX 76-120).

4. Conclusion

- In this study, computer code using MATLAB program, based on the double-multiple stream tube (DMST) model, has been utilized for indicating the aerodynamic loads and performance of H- type Darrieus VAWT.
- Computer code based on the DMST model was successfully validated by comparing it to the data provided by the research literature.
- The power coefficient and self-starting behaviors of four families of symmetric airfoils (NACA00XX, S, FX, and E) were compared for low tip-speed ratios ranging from 0 to 4.5 at a low wind speed of 4 m/s.
- It clearly shows that the symmetrical airfoil section s1046 is the best compared with other airfoils that have shown the best performance in other families such as NACA 0018, E169, and FX 76-120.

Authors' contribution

All authors contributed equally to the preparation of this article.

Declaration of competing interest

The authors declare no conflicts of interest.

Funding source

This study didn't receive any specific funds.

REFERENCES

- [1] R. Avtar, S. Tripathi, A. K. Aggarwal, and P. Kumar, "Population–Urbanization–Energy Nexus: A Review," *Resources*, vol. 8, no. 3, p. 136, 2019.
- [2] N. L. Panwar, S. C. Kaushik, and S. Kothari, "Role of renewable energy sources in Environmental Protection: A Review," *Renewable and Sustainable Energy Reviews*, vol. 15, no. 3, pp. 1513–1524, 2011.
- [3] J. Thé and H. Yu, "A critical review on the simulations of wind turbine aerodynamics focusing on hybrid RANS-LES Methods," *Energy*, vol. 138, pp. 257–289, 2017.
- [4] J. Liu, H. Lin, and J. Zhang, "Review on the technical perspectives and commercial viability of vertical axis wind turbines," *Ocean Engineering*, vol. 182, pp. 608–626, 2019.
- [5] X. Jin, G. Zhao, K. J. Gao, and W. Ju, "Darrieus Vertical Axis Wind Turbine: Basic Research Methods," *Renewable and Sustainable Energy Reviews*, vol. 42, pp. 212–225, 2015.
- [6] M. ISLAM, D. TING, and A. FARTAJ, "Aerodynamic models for various-type straight-bladed vertical axis wind turbines," *Renewable and Sustainable Energy Reviews*, vol. 12, no. 4, pp. 1087–1109, 2008.
- [7] J. V. Akwa, H. A. Vielmo, and A. P. Petry, "A review on the performance of Savonius Wind Turbines," *Renewable and Sustainable Energy Reviews*, vol. 16, no. 5, pp. 3054–3064, 2012.
- [8] Y. Li, "Straight-Bladed Vertical Axis Wind Turbines: History, Performance, and Applications." Available: <https://scholar.archive.org/work/lbnadrf3tjfm3fgyzu6fxuspbe/access/wayback/https://cdn.intechopen.com/pdfs/65843>
- [9] X. Cai, Y. Zhang, W. Ding, and S. Bian, "The aerodynamic performance of H-Type Darrieus VAWT rotor with and without winglets: CFD Simulations," *Energy Sources, Part A: Recovery, Utilization, and Environmental Effects*, pp. 1–12, 2019.

- [10] R. J. Templin, Aerodynamic performance theory for the NRC vertical-axis wind turbine. National Aeronautical Establishment, Ottawa, Ontario (Canada), 1974.
- [11] J. H. Strickland, "A performance prediction model for the Darrieus turbine." *International symposium on wind energy systems*, 1977.
- [12] I. Paraschivoiu, "Double-multiple streamtube model for Darrieus in turbines," *NASA. Lewis Research Center Wind Turbine Dyn.*, 1981
- [13] M. M. Aslam Bhutta, N. Hayat, A. U. Farooq, Z. Ali, Sh. R. Jamil, and Z. Hussain, "Vertical axis wind turbine – A review of various configurations and design techniques," *Renewable and Sustainable Energy Reviews*, vol. 16, no. 4, pp. 1926–1939, 2012.
- [14] N. Durrani, H. Hameed, H. Rahman, and S. Chaudhry, "A Detailed Aerodynamic Design and Analysis of a 2-D Vertical Axis Wind Turbine Using Sliding Mesh in CFD," *49th AIAA Aerospace Sciences Meeting including the New Horizons Forum and Aerospace Exposition*, 2011.
- [15] J. Castillo, "Small-scale vertical axis wind turbine design," *Tampere University of Applied Sciences*, 2011.
- [16] M. H. Mohamed, "Performance investigation of H-rotor Darrieus turbine with new airfoil shapes," *Energy*, vol. 47, no. 1, pp. 522–530, 2012.
- [17] F. Kanyako and I. Janajreh, "Numerical Investigation of Four Commonly Used Airfoils for Vertical Axis Wind Turbine," *ICREGA'14 - Renewable Energy: Generation and Applications*, pp. 443–454, 2014.
- [18] C.-C. Nguyen, H.-H. Li, and T. Phát, "A Numerical Study of Thickness Effect of the Symmetric NACA 4-Digit Airfoils on Self Starting Capability of a 1kW H-Type Vertical Axis Wind Turbine," *International Journal of Mechanical Engineering and Applications*. vol. 3, pp. 7–16, 2015.
- [19] A. Subramanian *et al.*, "Effect of airfoil and solidity on the performance of small scale vertical axis wind turbine using three dimensional CFD model," *Energy*, vol. 133, pp. 179–190, 2017.
- [20] Ion Paraschivoiu, "Aerodynamic Loads and Performance of the Darrieus Rotor," *Journal of Energy*, vol. 6, no. 6, pp. 406–412, 1982.
- [21] Paraschivoiu, Ion. Wind turbine design: with emphasis on the Darrieus concept. Presses inter Polytechnique, 2002.
- [22] The *US. standard Atmosphere, 1976*, United States Air Force, Washington, D.C.
- [23] M. Raciti Castelli, A. Englaro, and E. Benini, "The Darrieus Wind Turbine: Proposal for a new performance prediction model based on CFD," *Energy*, vol. 36, no. 8, pp. 4919–4934, 2011.
- [24] I. Paraschivoiu, O. Trifu, and F. Saeed, "H-Darrieus Wind Turbine with blade pitch control," *International Journal of Rotating Machinery*, vol. 2009, pp. 1–7, 2009.
- [25] B. Kirke, "Evaluation of self-starting vertical axis wind turbines for stand-alone applications," Ph.D. Thesis, Griffith University, 1998.